2024 IEEE International Conference on Robotics and Automation (ICRA 2024)
May 13-17, 2024. Yokohama, Japan

Tethered Lifting-Wing Multicopter Landing Like Kite

Haoyu Wei, Shuai Wang and Quan Quan

***Abstract*— Automatic landing of tethered unmanned aerial vehicles (UAVs) is an important issue. Typically, UAVs rely on location sensors such as global navigation satellite system (GNSS) and external cameras to obtain location data. However, harsh environments such as denial GNSS or strong winds make it difficult for UAVs to approach the landing area, and common solutions cannot be used for automatic landing. A tethered lifting-wing multicopter has a structure and static stability similar to a kite. Inspired by kites, this paper proposes a new landing method for tethered lifting-wing multicopters, which can be used without location or velocity sensors. During the landing phase, the tethered lifting-wing multicopter only needs to keep the rotor thrust to actively straighten the tethered cable and a constant attitude similar to that of a kite to keep position stability and increase damping. Meanwhile, the winch only needs to recover the cable at a constant speed until the tethered lifting-wing multicopter returns to its base. Real flight experiments demonstrate the feasibility and practicability of this method.**

Fig. 1. Landing experiment of the tethered lifting-wing multicopter conducted outdoors. The figure is composed of multiple photos to show the whole landing process.

I. INTRODUCTION

In recent years, technology development has led to the increasingly widespread application of unmanned aerial vehicles (UAVs) [1]. However, in tasks that require long hovering, such as emergency communications and lighting, common UAVs are incompetent due to their short endurance, so tethered UAVs are a choice. The tethered UAV is connected to the ground base station through a cable, which can play the role of data transmission and power supply [2]–[4]. Common tethered UAVs can be divided into tethered multicopters, tethered fixed wings, and kite-like aircraft. However, tethered multicopters have weak wind resistance and poor static stability; tethered fixed-wings and kite-like aircraft cannot vertically take off, land, or hover.

In the face of the problems existing in common tethered UAVs, lifting-wing multicopters can be employed in tethered unmanned systems to create tethered lifting-wing multicopters. The lifting-wing multicopter is a new kind of vertical takeoff and landing (VTOL) UAVs [5], [6]. Unlike traditional hybrid VTOL UAVs or tail-sitter VTOL UAVs, the mounting angle of the wing relative to the rotor is generally around 45 degrees for lifting-wing multicopters, which makes them have better static stability [7]. Tethered lifting-wing multicopters have both structures of tethered multicopters and kites. They can use rotors for vertical takeoff and landing, as well as use wings to provide wind energy and improve static stability.

Haoyu Wei, Shuai Wang, and Quan Quan (Corresponding Author) are with School of Automation Science and Electrical Engineering, Beihang University, Beijing, 100191, P.R. China wei_haoyu@buaa.edu.cn, wsh_buaa@buaa.edu.cn, qq_buaa@buaa.edu.cn.

This work was supported by the National Natural Science Foundation of China under Grant 61973015.

The landing of tethered UAVs on mobile platforms is an important issue. Typically, the UAV needs sensors such as the global navigation satellite system (GNSS) to obtain the position relative to the mobile platform [8]. In GNSS-denied environments, locating UAVs relies heavily on other external sensors. It is common to use external cameras to achieve precise landings by identifying the visual features of the landing area or using infrared guidance modules [9]–[11]. However, it is difficult to approach the landing area in strong winds for the UAV, so the area was outside the observation range of the camera, which led to the failure of the landing. Another method is sensing or measuring the length and angle of the tether cable to locate the UAV. However, it is difficult to measure accurately or require redundant sensors [12], [13].

Observing kites in daily life, it is found that they have many advantages in the recovery process. Firstly, they have good static stability [14], [15]. Secondly, they do not need external sensors to obtain location data. Lastly, the recovery of kites is absolutely accurate under the constraints of tethered cables. It is noted that tethered lifting-wing multicopters have a similar structure to kites. The wing has a similar pitch angle to the kite because of the installation angle, which makes them perform similarly [16].

Inspired by kites, this paper proposes a new method for tethered lifting-wing multicopters automatic landing on mobile platforms, which can be used only with onboard Inertial Measuring Unit (IMU) and without any location or velocity sensors. During the landing process, the tethered lifting-wing multicopter actively straightens the cable by increasing the rotor thrust in the altitude direction and keeps a constant attitude, forming a structure similar to a kite in the wind or an inverted pendulum, which can improve static

stability with the help of the taut cables. At the same time, the cable winch starts recovering the tethered cable at a constant speed. Finally, as the tethered cable is recovered, the tethered lifting-wing multicopter is dragged like a kite, completing the automatic landing. The main contributions of the paper are as follows.

- A new kite-like landing approach for tethered lifting-wing multicopters, including the lifting-wing multicopter control and the winch control. The control method is straightforward but reliable because (i) the tethered lifting-wing multicopter control imitates the control principle of a kite without any location or velocity sensors but obtaining stability; (ii) the winch control is also simple but works and is independent of the lifting-wing multicopter control by assigning slower dynamics.
- The real autonomous landing experiments without location or velocity sensors further demonstrate the feasibility and practicality of this approach.

II. PRELIMINARIES AND PROBLEM FORMULATION

A. Definition of Coordinate System

Tethered lifting-wing multicopters involve multiple coordinate systems, shown in Fig. 2.

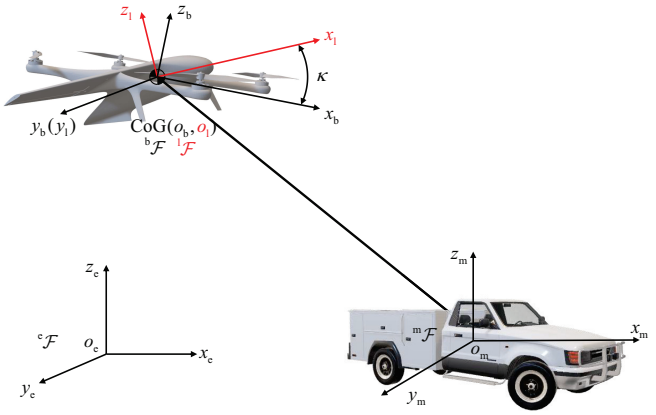

(a) Definition and relationship of ${}^e\mathcal{F}$, ${}^b\mathcal{F}$, and ${}^l\mathcal{F}$

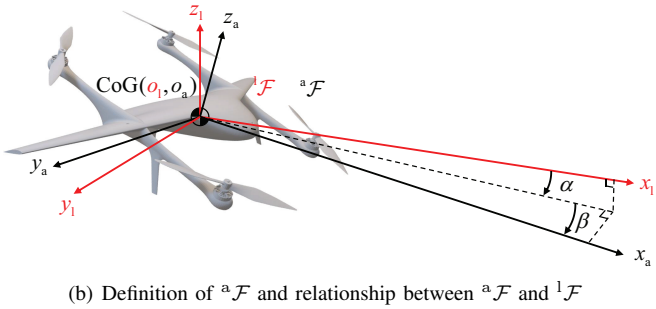

(b) Definition of ${}^a\mathcal{F}$ and relationship between ${}^a\mathcal{F}$ and ${}^l\mathcal{F}$

Fig. 2. Definition and Relationship of Coordinate Frames

Define the earth-fixed frame as ${}^e\mathcal{F}$, the lifting-wing frame as ${}^l\mathcal{F}$, the multicopter frame as ${}^b\mathcal{F}$, the mobile platform frame as ${}^m\mathcal{F}$, and the wind frame as ${}^w\mathcal{F}$. The frame ${}^m\mathcal{F}$ is parallel to ${}^e\mathcal{F}$. Coordinate points o_b, o_l and o_w are coincided with the center of gravity (CoG). The transformation from ${}^b\mathcal{F}$ to ${}^e\mathcal{F}$ is represented by the rotation matrix $\mathbf{R}_b^e$, which is expressed by Euler angles under Z-Y-X order as

$$\mathbf{R}_b^e = \begin{bmatrix} c\theta c\psi & s\phi s\theta c\psi - c\phi s\psi & c\phi s\theta c\psi + s\phi s\psi \\ c\theta s\psi & s\phi s\theta s\psi + c\phi c\psi & c\phi s\theta s\psi - s\phi c\psi \\ -s\theta & s\phi c\theta & c\phi c\theta \end{bmatrix} \tag{1}$$

where ϕ, θ and ψ denote the roll, pitch and yaw angle respectively. The transformation from ${}^l\mathcal{F}$ to ${}^b\mathcal{F}$ is represented by the rotation matrix $\mathbf{R}_l^b$, written as

$$\mathbf{R}_l^b = \begin{bmatrix} \cos\kappa & 0 & \sin\kappa \\ 0 & 1 & 0 \\ -\sin\kappa & 0 & \cos\kappa \end{bmatrix} \tag{2}$$

where κ is the installation angle of the wing relative to the rotor. The transformation from ${}^w\mathcal{F}$ to ${}^l\mathcal{F}$ is represented by the rotation matrix $\mathbf{R}_w^l$, written as

$$\mathbf{R}_w^l = \begin{bmatrix} \cos\alpha\cos\beta & -\cos\alpha\sin\beta & -\sin\alpha \\ \sin\beta & \cos\beta & 0 \\ \sin\alpha\cos\beta & -\sin\alpha\sin\beta & \cos\alpha \end{bmatrix} \tag{3}$$

where α is the angle of attack, and β is the angle of sideslip.

B. Dynamic Model of Tethered Lifting-Wing Multicopters

Considering the aerodynamic forces and tethered cable forces effect, based on the dynamic model of lifting-wing multicopters [7], the dynamic model in this paper is written as

$${}^e\dot{\mathbf{p}} = {}^e\mathbf{v} \tag{4}$$

$${}^e\dot{\mathbf{v}} = \frac{1}{m}\left({}^e\mathbf{T}_r + \mathbf{R}_b^e \cdot \mathbf{R}_l^b \cdot \mathbf{R}_w^l \cdot {}^w\mathbf{F}_a + {}^e\mathbf{F}_c\right) - \mathbf{g} \tag{5}$$

$$\dot{\mathbf{R}}_b^e = \mathbf{R}_b^e \left[{}^b\boldsymbol{\omega}\right]_\times \tag{6}$$

$${}^b\dot{\boldsymbol{\omega}} = \mathbf{J}^{-1}\left({}^b\boldsymbol{\tau}_r + {}^b\boldsymbol{\tau}_g + {}^b\boldsymbol{\tau}_c + \mathbf{R}_l^b \cdot {}^l\boldsymbol{\tau}_a - {}^b\boldsymbol{\omega} \times \mathbf{J} \cdot {}^b\boldsymbol{\omega}\right) \tag{7}$$

where ${}^e\mathbf{p}$, ${}^e\mathbf{v}$, $\mathbf{R}_b^e$ and ${}^b\boldsymbol{\omega}$ denote the position, velocity, orientation and angular rates of the tethered lifting-wing multicopter respectively. The matrix $\mathbf{J}$ is the inertia matrix of the tethered lifting-wing multicopter. Moments ${}^b\boldsymbol{\tau}_g$, ${}^l\boldsymbol{\tau}_a$, ${}^b\boldsymbol{\tau}_c$ and ${}^b\boldsymbol{\tau}_r$ denote the gyroscopic moment, the aerodynamic moment, the moment produced by the cable and the moment produced by rotors, respectively; $\mathbf{g}=[\,0 \quad 0 \quad g\,]^T$, and g is the gravity acceleration. Force ${}^w\mathbf{F}_a$ is the aerodynamic force in ${}^w\mathcal{F}$; ${}^e\mathbf{T}_r$ is the cable drag in ${}^e\mathcal{F}$; ${}^e\mathbf{F}_c$ is the rotor thrust in ${}^e\mathcal{F}$, written as

$${}^e\mathbf{F}_c = -\frac{F_c}{\|{}^m\mathbf{p}\|}{}^m\mathbf{p} \tag{8}$$

where $F_c = \|{}^e\mathbf{F}_c\|$ is the magnitude of the cable drag, ${}^m\mathbf{p}$ is the position of the tethered lifting-wing multicopter in ${}^m\mathcal{F}$.

C. Model of Cables and Cable Winches

The recovering speed of the cable v_c is expressed as the derivative of its length L. Considering the relationship between the recovering speed of cable v_c and the angular speed of the cable winch Ω_w, the model is written as

$$L = \|\mathbf{p}_e\| \tag{9}$$

$$\dot{L} = v_c \tag{10}$$

$$\Omega_w = \frac{v_c}{r} \tag{11}$$

where r is the radius of the cable winch.

The cable winch receives its own torque τ_w and cable drag F_c. When $\tau_w < 0$, the cable winch tends to recover the cable. Therefore, the model of cable winches is written as

$$J_w \dot{\Omega}_w = \tau_w + rF_c. \tag{12}$$

D. Problem Formulation

This paper aims to control tethered lifting-wing multicopters landing only with onboard IMUs. To simplify the problem, we make several assumptions.

Assumption 1: Cables are taut during recovering processes.

Remark 1: Tethered lifting-wing multicopters can actively straighten cables by increasing the thrust of rotors greater than gravity in the altitude direction [17]. On the one hand, straightened cables allow forces of cables to act directly on tethered lifting-wing multicopters during recovery. On the other hand, taut cables can improve the static stability of tethered lifting-wing multicopters [18], [19].

Assumption 2: The diameter of cable winches does not increase during recovering processes. And masses of cables are ignored. Cable drags act on the center of gravity of lifting-wing multicopters.

Remark 2: Cables are lightweight compared to tethered lifting-wing multicopters, and have a smaller diameter than cable winches. Therefore, the mass and diameter of cables can be ignored at lower heights.

Assumption 3: Winds acting on tethered lifting-wing multicopters are head-on, with $\beta = 0$.

Remark 3: The wing structure of lifting-wing multicopters makes them have good self-stability. If the lateral wind speed is small, the lateral force and the sideslip angle can be ignored to simplify the problem. In the case of high wind speeds, the tethered lifting-wing multicopter can self-stabilize in the direction of the wind [7], resulting in a slight sideslip angle that can also be ignored.

Based on the above assumptions, the problem to be solved in this paper is to design controllers that can be used only with onboard IMUs and without location or velocity sensors, which are respectively used on tethered lifting-wing multicopters and cable winches. The landing problem on mobile platforms is considered as follows.

Objective: Given an initial state ${}^{m}\mathbf{p}_{init}$, the current state ${}^{m}\mathbf{p}(t)$ and a time $T \geqslant 0$, design a control law that:

$$\begin{aligned} &\lim_{t\to\infty} \|{}^{m}\mathbf{p}(t)\| = 0 \\ &\text{s.t. } Eqs.\ (4), (5), (8), (9), (10),\ \forall t \in [0, \infty) \\ &\quad {}^{m}\mathbf{p}(0) = {}^{m}\mathbf{p}_{init} \end{aligned} \tag{13}$$

The position ${}^{m}\mathbf{p} = 0$ when $L = 0$. Therefore, the tethered lifting-wing multicopter can land on the mobile platform when cable recovery is complete.

III. KITE-INSPIRED LANDING CONTROLLER DESIGN

In this section, firstly, the stable mechanism of kites is discussed, and a kite-inspired controller is designed. Secondly, stability proof demonstrates that tethered lifting-wing multicopters exhibit similar stability to kites. Finally, the winch controller is designed.

The total control architecture is shown in Fig. 3.

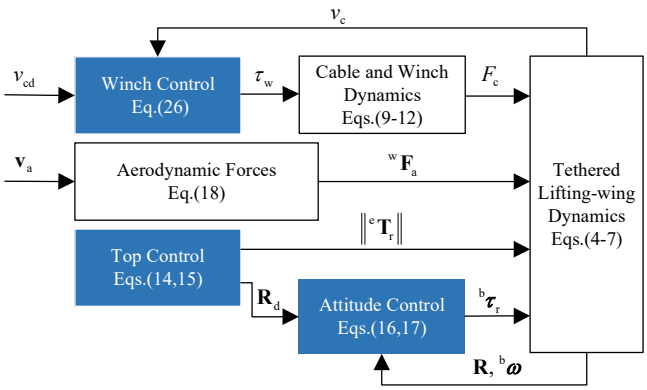

Fig. 3. Control closed-loop of the tethered lifting-wing multicopter

A. Tethered lifting-wing multicopters Landing Controller Design

The landing controller of lifting-wing multicopters is inspired by kites. Kites are only subjected to gravity, aerodynamic force, and cable pull in the air, with airlift greater than gravity. Therefore, kites are very similar to inverted pendulums because they can autonomously return to stable equilibrium points without external disturbance, shown in Fig. 4.

In the altitude direction, the lift is greater than gravity for kites. Therefore, they constantly move toward the highest points, and tethered cables can be actively straightened. In the horizontal direction, kites are naturally damping by wind resistance. When the kite has a forward speed, the velocity relative to the wind becomes larger, and the air resistance increases, thus forming a kind of velocity-negative feedback to keep the kite in equilibrium. Compared to tethered multicopters, the kite-like structure of tethered lifting-wing multicopters can increase aerodynamic lift and drag, thereby increasing damping and reducing oscillation.

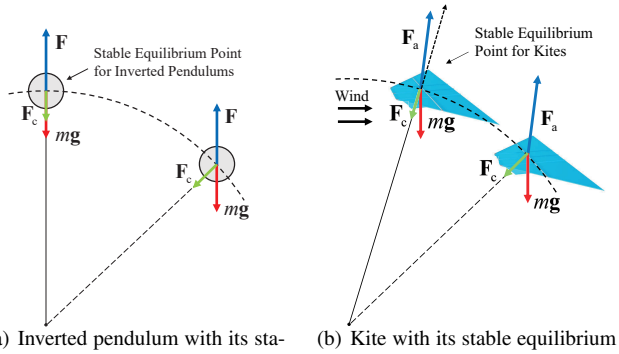

(a) Inverted pendulum with its stable equilibrium point

(b) Kite with its stable equilibrium point

Fig. 4. Kite is similar to inverted pendulum

Based on the above idea of kites, the tethered lifting-wing multicopter controller in the altitude direction is designed as

$$T_{\mathrm{r},z} = (1+\epsilon)\, mg \tag{14}$$

where $T_{\mathrm{r,z}}$ is the rotor thrust of the tethered lifting-wing multicopter in the altitude direction of ${}^{\mathrm{e}}\mathcal{F}$, ϵ is the proportion of additional gravity provided by rotors, m is the mass of the tethered lifting-wing multicopter.

In the horizontal direction, the lateral rotor thrust $T_{\mathrm{r},x}$ and $T_{\mathrm{r},y}$ are used to maintain attitude stability. Control quantity of the tethered lifting-wing multicopter is expressed as a 3-dimensional vector of thrust, written as

$${}^{\mathrm{e}}\mathbf{T}_{\mathrm{r}} = \begin{bmatrix} T_{\mathrm{r},x} & T_{\mathrm{r},y} & T_{\mathrm{r},z} \end{bmatrix}^{\mathrm{T}}. \tag{15}$$

Moreover, the attitude controller is designed. The reference angular rate ${}^{\mathrm{b}}\boldsymbol{\omega}_{\mathrm{d}}$ is written as

$${}^{\mathrm{b}}\boldsymbol{\omega}_{\mathrm{d}} = -\mathbf{K}_{\boldsymbol{\Theta}}\mathbf{e}_{\boldsymbol{\Theta}} \tag{16}$$

where $\mathbf{e}_{\boldsymbol{\Theta}} = \begin{bmatrix} \phi & \theta & \psi - \psi_{\mathrm{d}} \end{bmatrix}$, and $\mathbf{K}_{\boldsymbol{\Theta}}$ is angular feedback matrix. The angular rate controller is designed for Eq. 7, written as

$${}^{\mathrm{b}}\boldsymbol{\tau}_{\mathrm{r}} = \mathrm{sat}(-\mathbf{K}_{\mathrm{p}\boldsymbol{\omega}}\mathbf{e}_{\boldsymbol{\omega}} - \mathbf{K}_{\mathrm{i}\boldsymbol{\omega}}\int \mathbf{e}_{\boldsymbol{\omega}} - \mathbf{K}_{\mathrm{d}\boldsymbol{\omega}}\dot{\mathbf{e}}_{\boldsymbol{\omega}}, -\boldsymbol{\tau}_{\max}, \boldsymbol{\tau}_{\max}) \tag{17}$$

where $\mathbf{e}_{\boldsymbol{\omega}} = {}^{\mathrm{b}}\boldsymbol{\omega} - {}^{\mathrm{b}}\boldsymbol{\omega}_{\mathrm{d}}$; ${}^{\mathrm{b}}\boldsymbol{\tau}_{\mathrm{rd}}$ is reference rotor torque; $\mathbf{K}_{\mathrm{p}\boldsymbol{\omega}}$, $\mathbf{K}_{\mathrm{i}\boldsymbol{\omega}}$ and $\mathbf{K}_{\mathrm{d}\boldsymbol{\omega}}$ are angular rate feedback matrices.

Apart from that, the tethered lifting-wing multicopter is subjected to aerodynamic forces. Notably, the install angle κ is large and exceeds the common stall angle. Therefore, we consider aerodynamic forces as velocity-negative feedback, written as

$${}^{\mathrm{w}}\mathbf{F}_{\mathrm{a}} = -\rho S\boldsymbol{\Phi}\mathbf{v}_{\mathrm{a}} = \begin{bmatrix} F_D & F_Y & F_L \end{bmatrix}^{\mathrm{T}} \tag{18}$$

where F_D, F_Y and F_L denote the aerodynamic drag, lateral and lift force respectively, ρ is the air density, S is the wing area of the tethered lifting-wing multicopter, $\mathbf{v}_{\mathrm{a}}$ is the velocity of the tethered lifting-wing multicopter relative to the wind, written as

$$\mathbf{v}_{\mathrm{a}} = {}^{\mathrm{e}}\mathbf{v} - \mathbf{v}_{\mathrm{w}} \tag{19}$$

where $\mathbf{v}_{\mathrm{w}}$ is the air velocity.

In Eq. (18), the matrix $\boldsymbol{\Phi}$ is used to represent aerodynamic parameters, written as

$$\boldsymbol{\Phi} = \begin{bmatrix} C_D & 0 & 0 \\ 0 & C_Y & 0 \\ 0 & 0 & C_L \end{bmatrix} \tag{20}$$

where C_D, C_Y, and C_L denote the aerodynamic drag, lateral force, and lift coefficient, respectively.

B. Kite-like Stable Proof

In this subsection, we demonstrate that the tethered lifting-wing multicopter has the ability to autonomously return to a stable equilibrium point when using the kite-inspired controller in this paper.

Tethered lifting-wing multicopters can automatically align with the direction of the wind. At the same time, the tethered lifting-wing multicopter is only subjected to aerodynamic force and cable drag in the horizontal direction, so it can automatically align with the moving platform, shown in Fig. 5(a). The angle Γ is the angle between the cable and $o_{\mathrm{m}}z_{\mathrm{m}}$; $o_{\mathrm{m}}x_{\mathrm{mc}}$ is the projection of cable on the horizontal plane.

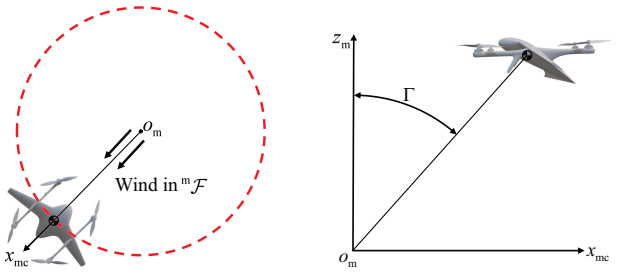

(a) Relationship between the direction of the tethered lifting-wing and the cable in the horizontal plane

(b) Longitudinal plane where the cable is located

Fig. 5. Tethered lifting-wing multicopter can automatically align with the moving platform.

Let the cable be recovered at a slowly constant speed, which is a slower dynamic process than the oscillation in the tangential direction of the cable. In this case, the two controls can be decomposed rather than mixed together to affect the stability of the whole system in theory. The scarification is the recovery speed. Since we ignore the effect of cable length changes on stability, this problem is analyzed in the mobile platform coordinate, which is considered as follows.

Problem: Given a stable equilibrium state $\mathbf{q}_{\mathrm{s}} = \begin{bmatrix} \Gamma_{\mathrm{s}} & 0 \end{bmatrix}^{\mathrm{T}}$, the current state $\mathbf{q} = \begin{bmatrix} \Gamma & \dot{\Gamma} \end{bmatrix}^{\mathrm{T}}$ and a time $T \geqslant 0$, it has:

$$\begin{aligned} &\lim_{t\to\infty} \|\mathbf{q} - \mathbf{q}_{\mathrm{s}}\| = 0 \\ &\text{s.t.} \quad Eqs.\ (5)(14)(18),\ \forall t \in [0, \infty). \end{aligned} \tag{21}$$

We choose the Lyapunov function as follows

$$V = \frac{1}{2}mL\dot{\Gamma}^2 + (1-\cos\Gamma)(\epsilon mg + F_{L0}) + (1-\sin\Gamma)(-F_{D0}) \tag{22}$$

where $F_{L0}>0$ and $F_{D0}<0$ denote the aerodynamic lift and drag force in a stable equilibrium state, respectively. Furthermore, taking the derivative of V yields

$$\dot{V} = \dot{\Gamma}mL\ddot{\Gamma} + \sin\Gamma(\epsilon mg + F_{L0}) + \cos\Gamma F_{D0}. \tag{23}$$

In the tangent direction of the cable, there is a dynamic model written as

$$\begin{aligned} mL\ddot{\Gamma} &= -(F_L + T_{\mathrm{r},z} - mg)\sin\Gamma - F_D\cos\Gamma \\ F_L &= F_{L0} + \rho S C_L L\dot{\Gamma}\sin\Gamma \\ F_D &= F_{D0} + \rho S C_D L\dot{\Gamma}\cos\Gamma. \end{aligned} \tag{24}$$

Substituting Eq. (24) into Eq. (23) results in

$$\dot{V} = -\rho S C_L \dot{\Gamma}^2 \sin^2\Gamma - \rho S C_D \dot{\Gamma}^2 \cos^2\Gamma \tag{25}$$

where $C_L>0$ and $C_D>0$. It is obtained that $\dot{V}<0$ when $\dot{\Gamma} \neq 0$. Since the Lyapunov function V is positively definite, while its derivative $\dot{V}$ is negative definite when $\dot{\Gamma} \neq 0$. We can conclude that $\dot{\Gamma} \to 0$ then $\Gamma_{\mathrm{s}} \to \Gamma$.

In summary, in the face of ***Problem***, the tethered lifting-wing multicopter can converge from the initial state $\mathbf{q}_{\mathrm{init}}$ to the target state $\mathbf{q}_{\mathrm{s}}$.

C. Cable Winched Controller Design

In this paper, the cable winch is controlled to recover the cable at a constant speed. For a real winch motor, the rotational angular speed and output torque of the motor are read and controlled, so it is necessary to design a controller that inputs the rotational angular speed of the motor and outputs the torque of the winch motor, written as

$$\begin{aligned} \tau_{\mathrm{w}} &= \epsilon mgr - k_{\mathrm{p}\Omega}e_\Omega - k_{\mathrm{i}\Omega}\int e_\Omega - k_{\mathrm{d}\Omega}\dot{e}_\Omega \\ e_\Omega &= \Omega_{\mathrm{w}} - \Omega_{\mathrm{wd}} \end{aligned} \tag{26}$$

where τ_{c} is the controlled output torque of the winch motor; $\Omega_{\mathrm{wd}} = v_{\mathrm{cd}}/r$ is the reference angular speed of the winch; Ω_{w} is the real angular speed of the winch; $k_{\mathrm{p}\Omega}$, $k_{\mathrm{i}\Omega}$ and $k_{\mathrm{d}\Omega}$ are feedback coefficients.

IV. SIMULATION AND REAL-WORLD EXPERIMENTS

In this section, we conduct simulations and outdoor real-world landing experiments of tethered lifting-wing multicopters. The results demonstrate that the controller designed in this paper can reliably complete the autonomous landing task only with onboard IMUs.

A. System Composition and Parameter Settings

The system consists of a mobile platform and a tethered lift-wing multicopter connected by a cable. Parameters of the tethered lift wing multicopter are shown in Table I.

TABLE I
PARAMETERS OF THE TETHERED LIFTING-WING MULTICOPTER

Explanation, Notation	Value
Mass of the tethered lifting-wing multicopter, m	1.2 kg
Inertia matrix of the lifting-wing multicopter, $\mathbf{J}$	diag (0.0126, 0.0055, 0.0158) kg$\cdot$ m^2
Lifting-wing installation angle, κ	0.59 rad
Wing area of the lifting-wing, S	0.09 m^2
Proportion of additional gravity provided by rotors, ϵ	0.2

TABLE II
ENVIRONMENT PARAMETERS FOR SIMULATION

Explanation, Notation	Value
Velocity of the Mobile Platform, ${}^{\mathrm{e}}\mathbf{v}_{\mathrm{m}}$	[1.4 1.4 0]$^{\mathrm{T}}$ m/s
Init Relative Position of the Tethered Lifting-wing Multicopter, ${}^{\mathrm{e}}\mathbf{p}(0)$	[-5 -5 10]$^{\mathrm{T}}$ m
Reference Recovering Speed of the Cable, v_{cd}	1 m/s
Wind Velocity, $\mathbf{v}_{\mathrm{w}}$	[-2 -2 0]$^{\mathrm{T}}$ m/s

B. Simulation

Before the real-world experiment, it is necessary to verify the reliability of the controller through simulation. We set several simulation environment parameters, shown in Table II.

The detailed state data of the tethered lifting-wing multicopter and the reference mobile platform in the simulation is shown in Fig. 6(a). The whole landing process observed from the side of the simulation is shown in Fig. 6(b). Based on the simulation, it is observed that the controller can complete the landing task reliably.

C. Real-World Experiment Results

1) Hardware: The Hardware used in experiments is shown in Fig. 7.

The cable winch is mounted on the mobile platform. Because a large torque may be generated during the landing process, a motor with a planetary gearbox is required as the winch motor in the experiment [20]. Therefore, we use the GO-M8010-6 motor produced by Unitree Technology.

The lifting-wing part of the tethered lifting-wing multicopter is machined from expanded polypropylene (EPP) foam and connected to the multicopter body by a 3D-printing connector with a fixed installation angle. The power system includes a 1300mAh six-cell lithium polymer (LiPo) battery, Tmotor F60PROV-LV motors, GF51499-3 propellers, and a Tmotor F55A electronic speed control (ESC). A Pixhawk4 flight controller is mounted in the center, with a barometer on the board to provide altitude and an inertial measurement unit (IMU) to provide Euler angles. A set of GNSS is installed only to record data.

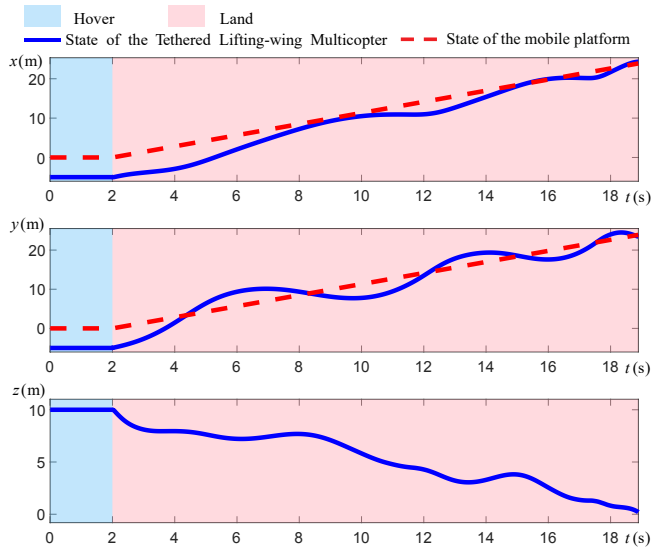

(a) Detailed data in landing process of the tethered lifting-wing multicopter

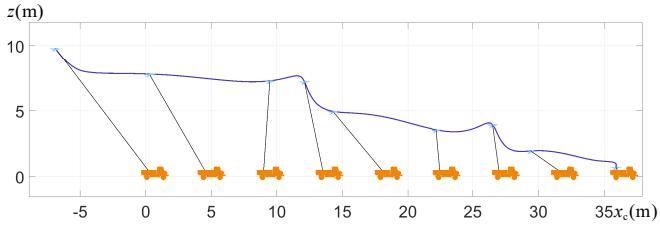

(b) Landing process observed from the side

Fig. 6. Landing process in simulation, x_c is the moving direction of the mobile platform

Fig. 7. Hardware used in experiments

The controller designed in this paper is built on the MATLAB/Simulink platform, which is automatically generated and uploaded to the Pixhawk4 board through the RflySim toolchain [21], [22].

2) Experiment Results: Sets of experiments verify the feasibility and reliability of the controller. We set the initial length of the cable as $L(0) = 3$m.

The whole landing process is shown in Fig. 1. The detailed location and velocity data of the tethered lifting-wing multicopter and the mobile platform are shown in Fig. 8.

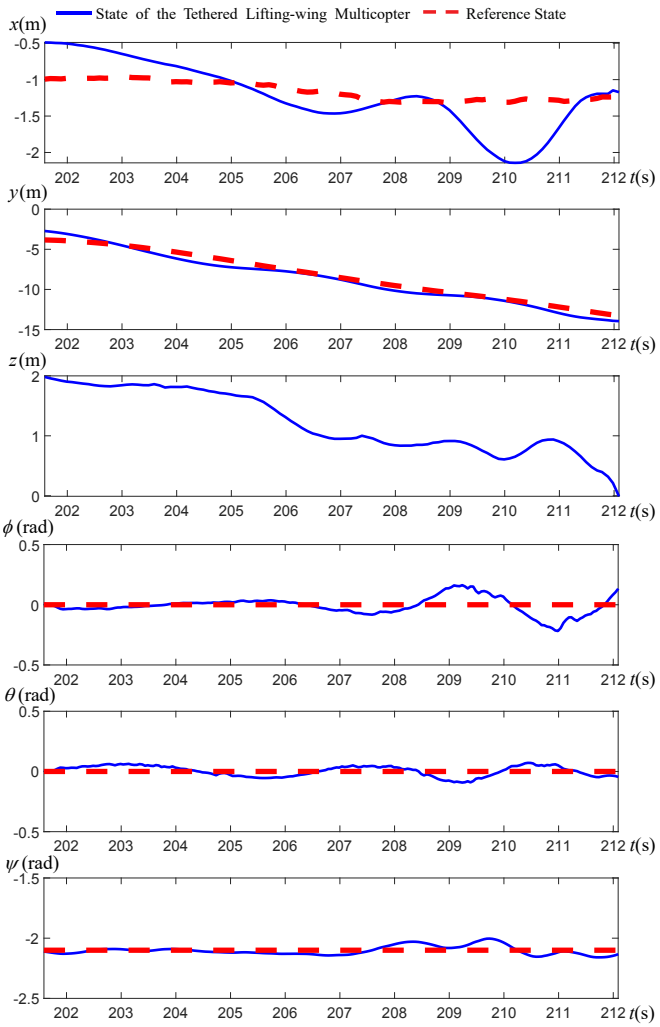

Fig. 8. Process of the real-world landing experiment

From the experimental results, it is found that the tethered lifting-wing multicopter can track the position and velocity of the moving platform under the drag of the cable, although there is an error in the initial position. It can complete the autonomous landing successfully.

V. CONCLUSIONS

In this paper, a kite-inspired tethered lifting-wing multicopter automatic landing controller is designed, which is used without location sensors (only with onboard IMUs). The kite-like stability proof is made. Simulation and real-world flight experiments are provided to show the feasibility and reliability of the proposed method. In the future, the cooperative control of the lifting-wing multicopter and winch deserves to be studied to improve the landing speed and transient process.

REFERENCES

[1] Q. Quan, *Introduction to Multicopter Design and Control*. Springer, 2017.

[2] A. Saif, K. Dimyati, K. A. Noordin, N. S. M. Shah, S. H. Alsamhi, and Q. Abdullah, "Energy-efficient tethered UAV deployment in B5G for smart environments and disaster recovery," in *2021 1st International Conference on Emerging Smart Technologies and Applications (eSmarTA)*, 2021, pp. 1–5.

[3] M. A. Kishk, A. Bader, and M.-S. Alouini, "On the 3-D placement of airborne base stations using tethered UAVs," *IEEE Transactions on Communications*, vol. 68, no. 8, pp. 5202–5215, 2020.

[4] B. Houska and M. Diehl, "Robustness and stability optimization of power generating kite systems in a periodic pumping mode," in *2010 IEEE International Conference on Control Applications*, 2010, pp. 2172–2177.

[5] K. Xiao, Y. Meng, X. Dai, H. Zhang, and Q. Quan, "A lifting wing fixed on multirotor UAVs for long flight ranges," in *2021 International Conference on Unmanned Aircraft Systems (ICUAS)*, 2021, pp. 1605–1610.

[6] H. Zhang, S. Tan, Z. Song, and Q. Quan, "Performance evaluation and design method of lifting-wing multicopters," *IEEE/ASME Transactions on Mechatronics*, vol. 27, no. 3, pp. 1606–1616, 2021.

[7] Q. Quan, S. Wang, and W. Gao, "Lifting-wing quadcopter modeling and unified control," *arXiv preprint arXiv:2301.00730*, 2023.

[8] Y. Kang, B.-J. Park, A. Cho, C.-S. Yoo, Y. Kim, S. Choi, S.-O. Koo, and S. Oh, "A precision landing test on motion platform and shipboard of a tilt-rotor UAV based on RTK-GNSS," *International Journal of Aeronautical and Space Sciences*, vol. 19, pp. 994–1005, 2018.

[9] J. L. Sanchez-Lopez, S. Saripalli, P. Campoy, J. Pestana, and C. Fu, "Toward visual autonomous ship board landing of a VTOL UAV," in *2013 International Conference on Unmanned Aircraft Systems (ICUAS)*, 2013, pp. 779–788.

[10] A. Paris, B. T. Lopez, and J. P. How, "Dynamic landing of an autonomous quadrotor on a moving platform in turbulent wind conditions," in *2020 IEEE International Conference on Robotics and Automation (ICRA)*, 2020, pp. 9577–9583.

[11] H. Lee, S. Jung, and D. H. Shim, "Vision-based UAV landing on the moving vehicle," in *2016 International Conference on Unmanned Aircraft Systems (ICUAS)*, 2016, pp. 1–7.

[12] L. Sandino, D. Santamaria, M. Bejar, A. Viguria, K. Kondak, and A. Ollero, "Tether-guided landing of unmanned helicopters without GPS sensors," in *2014 IEEE International Conference on Robotics and Automation (ICRA)*, 2014, pp. 3096–3101.

[13] X. Xiao, Y. Fan, J. Dufek, and R. Murphy, "Indoor UAV localization using a tether," in *2018 IEEE International Symposium on Safety, Security, and Rescue Robotics (SSRR)*, 2018, pp. 1–6.

[14] A. Pastor-Rodríguez, G. Sanchez-Arriaga, and M. Sanjurjo-Rivo, "Modeling and stability analysis of tethered kites at high altitudes," *Journal of Guidance, Control, and Dynamics*, vol. 40, no. 8, pp. 1892–1901, 2017.

[15] L. Salord Losantos and G. Sánchez-Arriaga, "Flight dynamics and stability of kites in steady and unsteady wind conditions," *Journal of Aircraft*, vol. 52, no. 2, pp. 660–666, 2015.

[16] H. Wei, S. Wang, and Q. Quan, "Modeling and longitudinal stability analysis of tethered lifting-wing quadcopters," in *2023 42nd Chinese Control Conference (CCC)*, 2023, pp. 4201–4206.

[17] L. Yang, G.-X. Du, Y. Gao, and Q. Quan, "Position control of tethered UAV with onboard inertial sensors," in *2022 41st Chinese Control Conference (CCC)*, 2022, pp. 2870–2875.

[18] S. Lupashin and R. D'Andrea, "Stabilization of a flying vehicle on a taut tether using inertial sensing," in *2013 IEEE/RSJ International Conference on Intelligent Robots and Systems (IROS)*, 2013, pp. 2432–2438.

[19] M. M. Nicotra, R. Naldi, and E. Garone, "Nonlinear control of a tethered UAV: The taut cable case," *Automatica*, vol. 78, pp. 174–184, 2017.

[20] H. Lee and Y. Choi, "A new actuator system using dual-motors and a planetary gear," *IEEE/ASME Transactions on Mechatronics*, vol. 17, no. 1, pp. 192–197, 2012.

[21] S. Wang, X. Dai, C. Ke, and Q. Quan, "RflySim: A rapid multicopter development platform for education and research based on pixhawk and matlab," in *2021 International Conference on Unmanned Aircraft Systems (ICUAS)*, 2021, pp. 1587–1594.

[22] Q. Quan, X. Dai, and S. Wang, *Multicopter Design and Control Practice: A Series Experiments Based on MATLAB and Pixhawk*. Springer Nature, 2020.